BULLETIN OF THE POLISH ACADEMY OF SCIENCES
TECHNICAL SCIENCES, Vol. 69(1), 2021, Article number: e135834
DOI: 10.24425/bpasts.2021.135834

Estimation of random bio-hydrodynamic lubrication parameters for joints with phospholipid bilayers

Krzysztof WIERZCHOLSKI[1*] and Andrzej MISZCZAK[2]

[1] WSG University of Economy in Bydgoszcz, ul. Garbary 2, 85-229 Bydgoszcz, Poland
[2] Gdynia Maritime University, ul. Morska 81/87, 81-225 Gdynia, Poland

Abstract. This paper presents a new form of a mathematical estimation of stochastic bio-hydrodynamic lubrication parameters for real human joint surfaces with phospholipid bilayers. In this work, the authors present the analytical and stochastic considerations, which are based on the measurements of human joint surfaces. The gap is restricted between two cooperating biological surfaces. After numerous experimental measurements, it directly follows that the random symmetrical as well as unsymmetrical increments and decrements of the gap height in human joints influence the hydrodynamic pressure, load-carrying capacity, friction forces, and wear of the cooperating cartilage surfaces in human joints. The main focus of the paper was to demonstrate the influence of variations in the expected values and standard deviation of human joint gap height on the hydrodynamic lubrication parameters occurring in the human joint. It is very important to notice that the new form of apparent dynamic viscosity of synovial fluid formulated by the authors depends on ultra-thin gap height variations. Moreover, evident connection was observed between the apparent dynamic viscosity and the properties of cartilage surface coated by phospholipid cells. The above observations indicate an indirect impact of stochastic changes in the height of the gap and the indirect impact of random changes in the properties of the joint surface coated with the phospholipid layers, on the value of hydrodynamic pressure, load carrying capacity and friction forces. In this paper the authors present a synthetic, comprehensive estimation of stochastic bio-hydrodynamic lubrication parameters for the cooperating, rotational cartilage bio-surfaces with phospholipid bilayers occurring in human joints. The new results presented in this paper were obtained taking into account 3D variations in the dynamic viscosity of synovial fluid, particularly random variations crosswise the film thickness for non-Newtonian synovial fluid properties. According to the authors' knowledge, the obtained results are widely applicable in spatiotemporal models in biology and health science.

Key words: human joint; estimation of lubrication parameters; phospholipid bilayer; analytical stochastic principles and solutions; apparent viscosity dependent on gap height random variations.

1. Introduction

The superficial layer of articular cartilage and the overlaying phospholipid bilayer membrane, only several nanometres thick, shape the height of the human joint gap [1–3]. Based on the numerous recent studies conducted with the use of an atomic force microscope (AFM), it was established that the phospholipid layer is not static [4]. The dimensions of the surface coated with phospholipids (PLs) and total joint gap height ε_T are generally subject to several unforeseeable repeated stochastic changes in relation to the nominal mean value. Random changes can be caused by micro vibrations, discrete joint load, or changes in roughness geometry. Another cause of random gap height changes is also the genetic and volumetric growth of live cells on the surface of cartilage with a phospholipid layer. Such small random changes are very significant [5–7]. The numerous previous experimental studies on the scope of the influence of the phospholipid membrane on the hydrodynamic process of surface lubrication were mainly focused on non-stochastic theory and experiments in the field of chemistry, without taking into account random changes [8–19]. There has been no previous stochastic research concerning frictional forces and coefficients of friction based on experimental methods and analytical-numerical hydrodynamics for lamellar and laminar biological flows [12, 17, 20, 21].

Occasional and few research efforts to date have been limited only to the influence of random joint gap height changes on pressure distribution. This fact inspired the authors to conduct bio-tribological research with a comprehensive approach to the stochastic changes in gap height as well as the velocity and viscosity of synovial fluid affecting pressure, load-carrying capacity of the joint, frictional force, and coefficient of friction.

Random studies require the selection of the most probable value for the changes under consideration. For this purpose, the expected value is determined for the gap height function, the surface coated with a phospholipid bilayer, and viscosity. The expected value is then the most probable value for joint gap height and viscosity. This value is necessary to determine joint lubrication parameters, in particular the hydrodynamic pressure, frictional forces, and coefficient of friction. The probabilistic description of the friction and lubrication process still requires the determination of standard deviations for the parameters discussed above.

*e-mail: krzysztof.wierzcholski@wp.pl

Manuscript submitted 2019-10-20, revised 2020-06-30, initially accepted for publication 2020-10-29, published in February 2021

Standard deviation intervals provide information about the possible range within which the location of the expected value may change. Random joint gap height changes have a direct and indirect influence on lubrication parameters such as pressure, joint load-carrying capacity, and friction forces. The direct influence is demonstrated by integral formulas determining lubrication parameters in the area of the lubricating layer. The indirect influence of random gap height changes on the value of lubrication parameters takes place through random changes in the dynamic viscosity of synovial fluid, which randomly affects changes in friction forces and pressure. In order to explain this phenomenon, it is necessary to take into account the fact that together with a random increase (decrease) in gap height, the flow velocity of synovial fluid in the gap decreases (increases). This results in a decrease (increase) in shear rate. Since synovial fluid has non-Newtonian properties, dynamic viscosity will eventually increase (decrease). Moreover, the indirect influence of random changes in the surface of articular cartilage coated with PLs on the value of lubrication parameters takes place through random changes in the dynamic viscosity of synovial fluid, which randomly affects changes in friction forces and pressure. In order to explain this phenomenon, it is necessary to consider the fact that apparent viscosity of synovial fluid η_T in the joint gap increases (decreases) together with increasing (decreasing) surface of cartilage coated with PLs [3,22–24].

The concentration of PLs in the superficial layer of the surface flowed around and the degree of wettability of these surfaces has a significant influence on the change of the viscosity of the physiological fluid accumulated in the boundary areas as well as on the changes in the values of the frictional forces, load-carrying capacity of the joint, and coefficient of friction [13]. Viscosity changes not only in the direction of the length and width of the flow – significant changes in viscosity are also revealed in the direction of the nanometre thickness of the layer.

The aim of the research undertaken in this work is the following:

1) to directly and indirectly explain the influence of the randomly changing gap height of human joints on the values of the viscosity and flow velocity of synovial fluid as well as on the values of hydrodynamic pressure and friction forces,
2) to show the analytical and numerical solutions for stochastic hydrodynamic lubrication of human joint with the use of experimental measurements implementation of random changes of joint gap height,
3) to present and to specify the inequalities, which determine the estimated values of the expected functions describing the basic bio-tribological parameters.

2. Random tools and materials for the performed research

The variety of curvature shapes of the analysed joint surfaces dictates the description of the surface in a curvilinear orthogonal coordinate system: α_1, α_2, α_3, where α_1 – circumferential direction of the rotational surface, α_3 – longitudinal direction, α_2 – gap height direction.

The joint gap is filled with synovial fluid. We assume characteristic constant dimensional joint gap height value ε_0 and dimensionless gap height function ε_{T1} dependent on variables α_1 and α_3. This function is the sum of two parts described by formula (1) [3]:

$$\varepsilon_{T1} = \varepsilon_T/\varepsilon_0 = \varepsilon_{T1s}(\alpha_1,\alpha_3)\,[1+\delta_1(\alpha_1,\alpha_3)]\,. \tag{1}$$

The symbol ε_{T1s} denotes the dimensionless gap height limited by the nominally smooth surfaces of articular cartilage. The changes of the gap height ε_T are caused by random hyperelastic deformations of articular cartilage as well as random protrusions of cartilage surface roughness. The dimensionless random variable of corrections for gap height is marked with the symbol δ_1. The expected value for the random variable of corrections δ_1 is defined by formula (2a), and the expected function for the entire gap height – by formula (2b) [25,26]:

$$EX(\delta_1) = \int_{-\infty}^{+\infty} (\delta_1)\times f(\delta_1)\,\mathrm{d}\delta_1\,, \tag{2a}$$

$$EX(\varepsilon_{T1}) = EX\,[\varepsilon_{T1s}\,(1+\delta_1)] = \varepsilon_{T1s}\,[1+EX(\delta_1)]\,. \tag{2b}$$

The symbol EX denotes the operator of the expected function. Probability density function f assigns probability values to the random variables of correction δ_1.

The ordinates of density function f are probabilities established for the random corrections δ_1 of joint gap height. These values were determined experimentally and take into account the articular cartilage roughness.

Standard deviation σ, from random variable of corrections, is determined with the use of the following formula [25,26]:

$$\sigma \equiv \sqrt{EX(\delta_1)^2 - EX^2(\delta_1)}. \tag{3}$$

Apart from gap height ε_T, phospholipid-coated surfaces, apparent dynamic viscosity η_T, hydrodynamic pressure, temperature, and other values are also subject to random change corrections.

The surface structure of the tested samples is irregular due to the occurrence of random roughness (from 10 to 50 nm) or disease [27].

Based on the comparisons made between the random changes in the rough cartilage surface structure measured in Cwanek's research [1] and Dowson's measurements [2], the probability density function is found to be unsymmetrical. This means that in most cases the probabilities of random increases in gap height are not equal to the probabilities of decreases in gap height.

The measurements of the random height changes in the surface roughness on cooperating joint surfaces were conducted using a sample (10 mm × 10 mm) of diseased cartilage taken from a human femoral head. See Fig. 1a, Fig. 1b. The measurements were carried out using a laser micro-sensor installed in a Rank Taylor Hobson-Talyscan 150 apparatus. The results were compiled using TalymapExpert and Microsoft Excel computer software. The measured gap height limited by the rough surfaces of the articular cartilage of the femoral head varied from 0.05 mm to 0.25 mm [1].

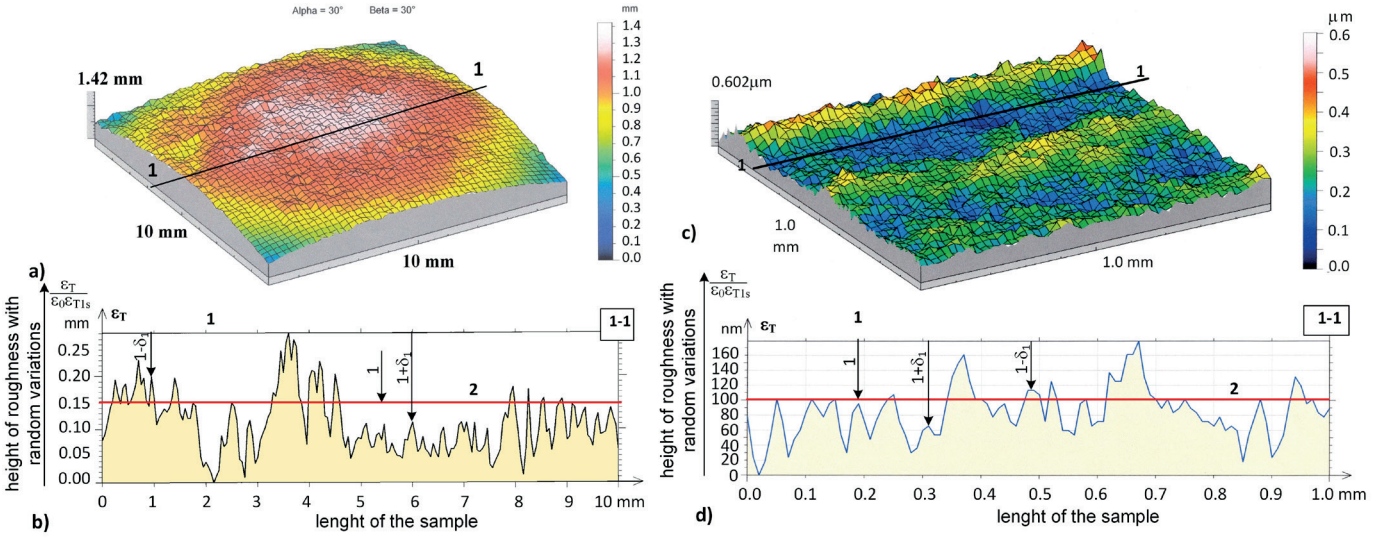

Fig. 1. Random changes in the surface structure and height ε_T of the joint gap caused by hyper-elastic deformations, unsteady load, and diseases, which enable the determination of random changes δ_1 in joint gap height: for sample a) (10 mm × 10 mm) and c) for sample (1.0 mm × 1.0 mm); b) random joint gap changes for cartilage, d) random joint gap changes for endoprosthesis; 1 – central axis of the height of a gap with smooth surfaces, 2 – smooth surface limiting the gap without random changes

3. Basic theoretical random methods

The stochastic vector equation for the conservation of momentum, continuity equation, energy conservation equation, Maxwell equations, Young-Kelvin-Laplace equation are written in the following directions: α_1, α_2, α_3 see Appendix. We take into account the expected functions of hydrodynamic pressure $EX[p(\alpha_1,\alpha_3)]$, temperature $EX[T(\alpha_1,\alpha_2,\alpha_3)]$, velocity of synovial fluid $EX[v_i(\alpha_1,\alpha_2,\alpha_3)]$, viscosity of lubricating fluid $EX[\eta_T(\alpha_1,\alpha_2,\alpha_3)]$, joint gap height $EX[\varepsilon_T(\alpha_1,\alpha_3)]$. We assume the incompressibility of biological fluid and ignore the influence of changes in the density of bio-fluid on changes in the equation for synovial fluid flow continuity. We use the known dependences between interfacial energy γ [mN/m] and power of hydrogen ion concentration pH and wettability We [14–18]. We take into account the influence of electrostatic field on the viscosity of bio-fluids studied by the authors [23]. Then we apply the classic simplification of hydrodynamic equations in the boundary layer by omitting the terms of the order of relative radial clearance with a value of 10^{-4}. Relative radial clearance is defined as the ratio of the thickness of the thin bio-fluid layer to the curvature radius of the rotational surface flowed around. After performing the transformations and calculations, we obtain the following stochastic equation system of hydrodynamic lubrication theory, taking PLs into account (44)–(49) [3, 22, 23, 28]:

$$0 = -\frac{1}{h_1}\frac{\partial EX(p)}{\partial \alpha_1} + \frac{\partial}{\partial \alpha_2}\left\{EX\left[\eta_T(\alpha_1,\alpha_2,\alpha_3)\right]\frac{\partial EX(v_1)}{\partial \alpha_2}\right\} + \rho_e E_1\,, \tag{4}$$

$$0 = \frac{\partial EX(p)}{\partial \alpha_2}\,, \tag{5}$$

$$-\frac{\rho EX\left(v_1^2\right)}{h_1 h_3}\frac{\partial h_1}{\partial \alpha_3} = -\frac{1}{h_3}\frac{\partial EX(p)}{\partial \alpha_3} + \frac{\partial}{\partial \alpha_2}\left\{EX\left[\eta_T(\alpha_1,\alpha_2,\alpha_3)\right]\frac{\partial EX(v_3)}{\partial \alpha_2}\right\} + \rho_e E_3\,, \tag{6}$$

$$\frac{1}{h_1}\frac{\partial EX(v_1)}{\partial \alpha_1} + \frac{\partial EX(v_2)}{\partial \alpha_2} + \frac{1}{h_1 h_3}\frac{\partial\left[h_1 EX(v_3)\right]}{\partial \alpha_3} = 0, \tag{7}$$

$$\frac{\partial}{\partial \alpha_2}\left\{\kappa\frac{\partial EX\left[T(\alpha_1,\alpha_2,\alpha_3)\right]}{\partial \alpha_2}\right\} + EX\left[\eta_T(\alpha_1,\alpha_2,\alpha_3)\right]\left\{\left[\frac{\partial EX(v_1)}{\partial \alpha_2}\right]^2 + \left[\frac{\partial EX(v_3)}{\partial \alpha_2}\right]^2\right\} = \frac{\boldsymbol{J}^2}{\sigma_e}\,, \tag{8}$$

where the expected function of apparent viscosity η_T [Pas] by virtue of (50) [22, 26] is:

$$EX\left[\eta_T(\alpha_1,\alpha_2,\alpha_3)\right] = EX\left[\eta_T(n,pH,We,T,\gamma,E)\right] \equiv \frac{\gamma_{\max}(pH,We) + kEX(A^{-1})\cdot EX(T)\ln L}{\delta_v \cdot EX(v_0)} \times \left[1+\delta_E(pH,E)E^2\right] \times \left(\sqrt{\left(\frac{\partial EX(v_{11})}{\partial \alpha_{21}}\right)^2 + \left(\frac{\partial EX(v_{31})}{\partial \alpha_{21}}\right)^2}\right)^{n-1}, \tag{9a}$$

$$0 < L \equiv \frac{\left(\sqrt{L_k}+1\right)^2}{(L_a+1)(L_b+1)} < 1,$$
$$L_a \equiv \frac{K_a}{a_H^+}, \qquad L_b \equiv \frac{a_H^+}{K_b}, \qquad L_k \equiv L_a L_b, \tag{9b}$$
$$(L_a+1)(L_b+1) > \left(\sqrt{L_k}+1\right)^2.$$

for: $0 \le \alpha_1 \le 2\pi$, $-b \le \alpha_3 \le +b$, $0 \le \alpha_2 \le EX(\varepsilon_T)$.

It follows from formula (9a) that apparent viscosity η_T of synovial fluid in the joint gap increases (decreases) together with increasing (decreasing) boundary surfaces A [m^2] between areas of different phospholipid (PL) concentration, i.e., of different cartilage susceptibility for $10^{-16}\,\mathrm{m}^2 < \mathrm{A} < 10^{-14}\,\mathrm{m}^2$. The influence of surface A, which is difficult to measure, on fluid viscosity will be analysed stochastically in Section 6.

Similarly to formulas (1) and (2a), specifying random gap height changes, expected functions of pressure, temperature, and lubricating fluid velocity components, occurring in the system of Eqs. (4)–(8), take the following forms:

$$EX(p) = p[1+EX(\delta_p)], \quad EX(T) = T[1+EX(\delta_T)],$$
$$EX(v_i) = v_i[1+EX(\delta_{vi})] \quad \text{for } i = 1,2,3. \tag{10}$$

where the symbols δ_p, δ_T, δ_{vi} denote unknown random variables of pressure, temperature, and synovial fluid velocity component corrections. If the random variable of gap height corrections $\delta_1 = 0$, then also $\delta_p = \delta_T = \delta_{vi} = 0$. In this case $EX(\delta_p) = EX(\delta_T) = EX(\delta_{vi}) = 0$, therefore under assumption (10) we have: $EX(p) = p$, $EX(T) = T$, $EX(v_i) = v_i$ for $i = 1,2,3$. Thus, in this special case, the system of Eqs. (4)–(8) loses stochastic properties. Lamé coefficients h_i, $i = 1,2,3$ were assumed for typical curvilinear rotational bio-surfaces with a non-monotonic generating line, flowed around by a thin layer of bio-fluid [23].

For two arbitrary cooperating biological surfaces, we apply the curvilinear, orthogonal system of co-ordinates α_1, α_2, α_3 with the respective Lamé coefficients h_1, h_2, h_3. After the abovementioned boundary simplifications of the thin arbitrary, curvilinear, non-rotational non-parallel surfaces, it follows that $h_2 = 1$ and $h_1 = h_1(\alpha_1, \alpha_3)$, $h_3 = h_3(\alpha_1, \alpha_3)$. For example, this case is valid for jump joint, collar bone, blade bone. For the thin biological liquid layer restricted by the two rotational surfaces in α_1 direction and non-monotone generating line in α_3 direction then the Lamé coefficients follows: $h_2 = 1$, $h_1 = h_1(\alpha_3)$, $h_3 = h_3(\alpha_3)$ or $h_3 = 1$ for monotone generating line in α_3 direction. This case is valid for human elbow joint or hip joint.

Considering the authors' research in article [22] and including the results of numerous discussions with the authors of papers [13–15], in which they discuss the influence of chemical properties of joint tissues and joint fluids on hydrodynamic lubrication of the human joint, similarly, we take into account the influence of the human joint physical parameters on its hydrodynamic lubrication.

The following designations were assumed: components E_i [V/m] ($i = 1,2,3$) of the electric intensity vector in α_i direction, $EX(T)$ [K] – expected value of randomly variable temperature T of synovial fluid, $2b$ [m] – length in the longitudinal direction of the friction area, $k = 1.38054 \cdot 10^{-23}$ J/K – Boltzmann constant, δ_v – dimensionless random coefficient ($0.2 < \delta_v < 0.6$). The dynamic viscosity of the bio-fluid decreases when index δ_v increases from 0.2 to 0.6. After experiments [1, 5] the coefficient δ_v describes the concentration c_c of collagen fibres in the bio-fluid. For $\delta_v = 0.2$ we have $c_c = 100\,000$ mol/mm^3, while for $\delta_v = 0.6$ concentration equals $c_c = 100$ mol/mm^3. The dimensionless value of parameters L_a, L_b was determined by formula (9b). Since $0 < L < 1$ [22], thus $\ln L$ is a negative number, while it is always the case that $\gamma_{\max} > -kA^{-1}T\ln L$, where $-100 < \ln L < 10$. The symbol $0.03\ \mathrm{m/s} < \mathrm{v}_0 < 0.04\ \mathrm{m/s}$ denotes the characteristic dimensional value of linear velocity for the bio-surface being flowed around [22]. The term described by dimensionless functions v_{11}, v_{31} of velocity vector components v_1 [m/s], v_3 [m/s] in directions α_1, α_3 in formula (9a) is a result of dimensionless transformations, where $v_1 = v_0 v_{11}$, $v_3 = v_0 v_{31}$. The symbol n denotes dimensionless flow index ($0.8 < n < 1.2$), where for $n = 1$ we have Newtonian fluid.

The following was assumed: δ_E [m^2/V^2] – experimental coefficient of the influence of electrical intensity $\boldsymbol{E}$ and concentration of hydrogen ions pH in the bio-fluid on the dynamic viscosity of the bio-fluid. The value of coefficient δ_E [m^2/V^2] for the bio-fluid has not yet been accurately measured experimentally. We only know that for $E = 10$ V/m and $pH = 8$ we obtain $\delta_E = 0.0003$ m^2/V^2 [29]. It thus follows that the dimensionless increase in the dynamic viscosity of the bio-fluid resulting from the influence of electric field in the phospholipid layer is $1 + \delta_E E^2 = 1.03$, i.e., only 3%. Based on the estimations obtained, we can see that the direct influence of electric field in the tissue boundary layer is negligible.

Formula (9) was derived from known dependences $\gamma(pH, We)$ describing the relationship between power of hydrogen ion concentration pH and wettability We. Interfacial energy was analytically transformed into apparent dynamic viscosity of the lubricating fluid η_T. Such dependences are illustrated graphically in the work of [23] for two types of phospholipids, PC and PS, with dimensionless values for acid pKa and base pKb equilibrium constant. An increase in pKa enhances viscosity increases in interval $2 < pH < 4$ and enhances viscosity decreases in interval $4 < pH < 10$. Bio-fluid dynamic viscosity for PC and PS lipids increases with increasing power of hydrogen ion concentration pH to certain isoelectric point IP ($\gamma = 3.5$ mJ/m^2) with established values We, δ_v, T, v_0. A further increase in pH causes a decrease in dynamic viscosity. The dynamic viscosity of the bio-fluid decreases with decreasing wettability We at established values δ_v, T, v_0. Drops in wettability from 70° to 50° indicate a transition from the hydrophobic to hydrophilic properties of the bio-surfaces flowed around by the bio-fluid.

System of partial differential equations (4)–(8) determines the following expected functions of randomly variables unknowns, namely: three bio-fluid velocity vector components $EX[v_i(\alpha_1, \alpha_2, \alpha_3)]$ [m/s] for $i = 1,2,3$; hydrodynamic pressure $EX[p(\alpha_1, \alpha_3)]$ [Pa], temperature $EX[T(\alpha_1, \alpha_2, \alpha_3)]$ [K]. The term on the left side of Eq. (6) describes the centrifugal forces occurring during the cooperation of two bio-surfaces. These forces occur only when Lamé coefficient h_1 is a function of α_3.

This applies to the bio-surface resting on a bone head with a spherical, conical, parabolic, or elliptical shape, not a cylindrical shape, where coefficient h_1 is a constant value.

4. Integration methods of random lubrication for rotational surfaces

Integration of the system of Eqs. (4)–(8), describing the lubrication of two rotational bio-surfaces with the participation of phospholipids (PL) separated by a thin layer of biological fluid, will be carried out in curvilinear coordinates $(\alpha_1, \alpha_2, \alpha_3)$.

The lubricated rotational bio-surface on the femoral head performs a rotational motion with angular velocity ω, while the second bio-surface (acetabulum) is stationary and limits a gap filled with a layer of bio-fluid of randomly varying height ε_T. Therefore, we apply the following boundary conditions to the function components of expected randomly varying bio-fluid velocities $EX(v_1), EX(v_2), EX(v_3)$ in directions $\alpha_1,\ \alpha_2,\ \alpha_3$:

$$\begin{aligned} &EX(v_1) = \omega h_1 \quad \text{for } \alpha_2 = 0, \\ &EX(v_1) = 0 \quad \text{for } \alpha_2 = EX(\varepsilon_T), \end{aligned} \tag{11}$$

$$\begin{aligned} &EX(v_2) = 0 \quad \text{for } \alpha_2 = 0, \\ &EX(v_2) = 0 \quad \text{for } \alpha_2 = EX(\varepsilon_T), \end{aligned} \tag{12}$$

$$\begin{aligned} &EX(v_3) = 0 \quad \text{for } \alpha_2 = 0, \\ &EX(v_3) = 0 \quad \text{for } \alpha_2 = EX(\varepsilon_T). \end{aligned} \tag{13}$$

By applying condition (11) to the general solution of Eq. (4), we obtain the following form of the function of the expected randomly variable component of bio-fluid velocity vector in circumferential direction α_1 of the rotational movable bio-surface [24]:

$$EX\left[v_1(\alpha_1,\alpha_2,\alpha_3)\right] = \left(\frac{1}{h_1}\frac{\partial EX(p)}{\partial \alpha_1} - M_1\right) A_\eta + \\ + (1 - A_s)\,\omega h_1\,, \tag{14}$$

where subordinate functions A_s [1], A_η [m^4/Ns] are the following:

$$A_s(\alpha_1,\alpha_2,\alpha_3) \equiv \frac{\int\limits_0^{\alpha_2} \frac{1}{EX(\eta_T)}\,\mathrm{d}\alpha_2}{\int\limits_0^{EX(\varepsilon_T)} \frac{1}{EX(\eta_T)}\,\mathrm{d}\alpha_2},$$

$$A_\eta(\alpha_1,\alpha_2,\alpha_3) \equiv \int\limits_0^{\alpha_2} \frac{\alpha_2}{EX(\eta_T)}\,\mathrm{d}\alpha_2 + \\ - \frac{\left(\int\limits_0^{\alpha_2} \frac{1}{EX(\eta_T)}\,\mathrm{d}\alpha_2\right)\left(\int\limits_0^{EX(\varepsilon_T)} \frac{\alpha_2}{EX(\eta_T)}\,\mathrm{d}\alpha_2\right)}{\int\limits_0^{EX(\varepsilon_T)} \frac{1}{EX(\eta_T)}\,\mathrm{d}\alpha_2}, \tag{15}$$

where: $0 \le \alpha_1 \le 2\pi\theta_1$, $0 \le \theta_1 \le 1$, $-b \le \alpha_3 \le +b$, $0 \le \alpha_2 \le EX(\varepsilon_T)$, $EX(\varepsilon_T) = EX[\varepsilon_T(\alpha_1,\alpha_3)]$.

When substituting solution (14) to Eq. (6) and applying condition (13), we obtain the function of the expected randomly variable component of bio-fluid velocity vector in longitudinal direction α_3 of the rotational bio-surface:

$$EX\left[v_3(\alpha_1,\alpha_2,\alpha_3)\right] = \left(\frac{1}{h_3}\frac{\partial EX(p)}{\partial \alpha_3} - M_3\right) A_\eta + \\ - \frac{\rho}{h_1 h_3}\frac{\partial h_1}{\partial \alpha_3} A_p\,. \tag{16}$$

The last term on the right side of Eq. (16) describes the influence of the suction effect of the rotational bio-surface with a monotonically variable generating line on the distribution of bio-fluid velocity in the joint gap. This influence disappears when the bio-surface is cylindrical in shape, and the generating line is a straight line parallel to the axis of rotation. Moreover $M_i = \rho_e E_i$ [N/m^3] for $i = 1,3$ are electrical terms. The following function of centrifugal effects A_p [m^6/Ns^3] was assumed:

$$A_p(\alpha_1,\alpha_2,\alpha_3) \equiv \left(\frac{1}{h_1}\frac{\partial EX(p)}{\partial \alpha_1} - M_1\right)^2 A_{\rho 1}(\alpha_1,\alpha_2,\alpha_3) + \\ - 2\omega\left(\frac{\partial EX(p)}{\partial \alpha_1} - h_1 M_1\right) A_{\rho 2}(\alpha_1,\alpha_2,\alpha_3) + \\ + (\omega h_1)^2 A_{\rho 3}\big((\alpha_1,\alpha_2,\alpha_3)\,, \tag{17}$$

where auxiliary functions $A_{\rho i}$ are derived in paper [22].

Integration of continuity Eq. (7) for boundary condition (12), where $v_2 = 0$ for $\alpha_2 = 0$, gives the following form of the function of the expected randomly variable component of bio-fluid velocity in the direction of gap height α_2:

$$EX\left[v_2(\alpha_1,\alpha_2,\alpha_3)\right] = -\int\limits_0^{\alpha_2} \frac{1}{h_1}\frac{\partial EX(v_1)}{\partial \alpha_1}\,\mathrm{d}\alpha_2 + \\ - \int\limits_0^{\alpha_2} \frac{1}{h_1 h_3}\frac{\partial\left[h_1 EX(v_3)\right]}{\partial \alpha_3}\,\mathrm{d}\alpha_2\,. \tag{18}$$

Now we substitute functions (14)–(16) to solution (18). We apply boundary condition (12) in the form $EX(v_2) = 0$ for $\alpha_2 = EX(\varepsilon_T)$, i.e. to the component of bio-fluid velocity vector in the direction of gap height α_2. We obtain the following stochastically modified Reynolds equations determining expected function $EX[p(\alpha_1,\alpha_3)]$ of randomly variable hydrodynamic pressure:

$$\frac{1}{h_1}\frac{\partial}{\partial\alpha_1}\left[\left(\frac{\partial EX(p)}{\partial\alpha_1}-h_1M_1\right)\left(\int_0^{EX(\varepsilon_T)}A_\eta\,\mathrm{d}\alpha_2\right)\right]+$$
$$+\frac{1}{h_3}\frac{\partial}{\partial\alpha_3}\left[\frac{h_1}{h_3}\left(\frac{\partial EX(p)}{\partial\alpha_3}-h_3M_3\right)\left(\int_0^{EX(\varepsilon_T)}A_\eta\,\mathrm{d}\alpha_2\right)\right]+$$
$$-\frac{\rho}{h_3}\frac{\partial}{\partial\alpha_3}\left(\frac{\partial h_1}{h_3\partial\alpha_3}\int_0^{EX(\varepsilon_T)}A_p\,\mathrm{d}\alpha_2\right)=$$
$$=\omega h_1\frac{\partial}{\partial\alpha_1}\left[\int_0^{EX(\varepsilon_T)}A_s\,\mathrm{d}\alpha_2-EX(\varepsilon_T)\right]. \tag{19}$$

When substituting the expected functions of bio-fluid velocity vector components (14), (16) to energy equation (8), for a constant value of bio-fluid thermal conductivity κ, after transformations we obtain the following differential equation, enabling the determination of the expected function of randomly variable temperature:

$$\frac{\partial^2EX(T)}{\partial\alpha_2^2}+\frac{EX(\eta_T)}{\kappa}\left\{\left[\left(\frac{1}{h_3}\frac{\partial EX(p)}{\partial\alpha_3}-M_3\right)\frac{\partial A_\eta}{\partial\alpha_2}\right]^2+\right.$$
$$\left.+\left[\left(\frac{1}{h_1}\frac{\partial EX(p)}{\partial\alpha_1}-M_1\right)\frac{\partial A_\eta}{\partial\alpha_2}-\omega h_1\frac{\partial A_s}{\partial\alpha_2}\right]^2\right\}+$$
$$+\frac{EX(\eta_T)}{\kappa}\frac{\rho}{h_1h_3}\frac{\partial h_1}{\partial\alpha_3}\frac{\partial A_p}{\partial\alpha_2}\left[\frac{\rho}{h_1h_3}\frac{\partial h_1}{\partial\alpha_3}\frac{\partial A_p}{\partial\alpha_2}+\right.$$
$$\left.-2\left(\frac{1}{h_3}\frac{\partial EX(p)}{\partial\alpha_3}-M_3\right)\frac{\partial A_\eta}{\partial\alpha_2}\right]=\frac{M_T}{\kappa} \tag{20}$$

for: $0\le\alpha_1\le2\pi$, $-b\le\alpha_3\le+b$, $0\le\alpha_2\le EX(\varepsilon_T)$, and $M_T/\kappa=\boldsymbol{J}^2/\sigma_\kappa$ [K/m^2], $\sigma_\kappa=\sigma_e\cdot\kappa$.

Expected function of randomly varying pressure $EX(p)$ is determined from Eq. (19) assuming the value of atmospheric pressure p_A at the edges of lubrication area $\Omega(\alpha_1,\alpha_3)$:

$$\begin{aligned}&p(\alpha_1,\alpha_3)=p_A\quad\text{for}\ \ (\alpha_1,\alpha_3)\in\mathrm{Fr}\,\Omega,\\&\Omega\in(0\le\alpha_1\le\pi)\times(\pi/2\le\alpha_3\le\pi),\end{aligned} \tag{21}$$

where Fr – topological boundary set operator. In order to determine expected function of randomly variable temperature $EX[T(\alpha_1,\alpha_2,\alpha_3)]$ from second order differential Eq. (20), two boundary conditions are required. The decreases and increases in the expected function of temperature below and above characteristic temperature T_0 ultimately give constant temperature value f_c on the first bio-surface (movable) and variable unknown value of temperature changes $f_p(\alpha_1,\alpha_3)$ on the second bio-surface (immovable). Thus, the two searched boundary conditions are as follows:

$$EX\,[T(\alpha_1,\alpha_2,\alpha_3)]=T_0+f_c\quad\text{for}\ \ \alpha_2=0, \tag{22a}$$
$$EX\,[T(\alpha_1,\alpha_2,\alpha_3)]=T_0+f_p(\alpha_1,\alpha_3)\quad\text{for}\ \ \alpha_2=EX(\varepsilon_T). \tag{22b}$$

In order to determine unknown temperature function $f_p(\alpha_1,\alpha_3)$ on the surface of the acetabulum, we use the condition of transportation of heat flux density q_c from the bone head surface, through the bio-liquid layer, to the surface of the acetabulum. This condition has the following form:

$$\kappa\frac{\partial EX(T)}{\partial\alpha_2}=-q_c\quad\text{for}\ \ \alpha_2=0. \tag{22c}$$

The components of expected random functions of friction forces in curvilinear α_1, α_3 directions occurring in human joint gaps with a PL bilayer have the following forms:

$$EX(F_{R1})=\iint_\Omega\left(EX(\eta_T)\frac{\partial EX(v_1)}{\partial\alpha_2}\right)_{\alpha_2=EX(\varepsilon_T)}\cdot\,h_1h_3\,\mathrm{d}\alpha_1\,\mathrm{d}\alpha_3, \tag{23}$$

$$EX(F_{R3})=\iint_\Omega\left(EX(\eta_T)\frac{\partial EX(v_3)}{\partial\alpha_2}\right)_{\alpha_2=EX(\varepsilon_T)}\cdot\,h_1h_3\,\mathrm{d}\alpha_1\,\mathrm{d}\alpha_3, \tag{24}$$

where: $0\le\alpha_1\le2\pi\theta_1$, $0\le\theta_1\le1$, $-b\le\alpha_3\le+b$, $0\le\alpha_2\le EX(\varepsilon_T)$, $\Omega(\alpha_1,\alpha_3)$ – lubrication surface.

The expected value of joint load carrying capacity $\boldsymbol{C}$ [N] acting in the opposite direction to load $\boldsymbol{W}$ [N] is determined from the following dependence:

$$EX(C)=\left\{\left[\int_{-b}^{+b}\left(\int_0^{\alpha_k}EX[p(\alpha_1,\alpha_3)]h_1(\sin\alpha_1)\,\mathrm{d}\alpha_1\right)\mathrm{d}\alpha_3\right]^2+\right.$$
$$\left.+\left[\int_{-b}^{+b}\left(\int_0^{\alpha_k}EX[p(\alpha_1,\alpha_3)]h_1(\cos\alpha_1)\,\mathrm{d}\alpha_1\right)\mathrm{d}\alpha_3\right]^2\right\}^{0.5}, \tag{25}$$

for $0\le\alpha_1\le\alpha_k<2\pi$, $-b\le\alpha_3\le+b$, $EX(\varepsilon_T)=EX[\varepsilon_T(\alpha_1,\alpha_3)]$, where: α_k denotes the bio-fluid end coordinate in circumferential direction α_1 of the femoral head, $2b$ – length in the longitudinal direction of the friction area.

The symbol $EX(p)$ denotes the expected function of the randomly variable hydrodynamic pressure function. Based on the Coulomb's law of friction, taking into account curvilinear orthogonal coordinate system, the dimensionless, randomly variable coefficient of friction has the following form:

$$\mu=\frac{|\boldsymbol{e}_1EX(F_{R1})+\boldsymbol{e}_3EX(F_{R3})|}{EX(C)}, \tag{26}$$

where $\boldsymbol{e}_1$, $\boldsymbol{e}_3$ are the unit vectors in circumferential α_1 and longitudinal α_3 directions.

5. Examples of geometrical description methods of rotational surfaces

The geometry of cylindrical biosurface is manifested in following example.

Let us consider the human elbow joint with two cooperating cylindrical rotational surfaces. Lower surface (bone head) moves in α_1 direction with angular velocity ω. Upper surface (acetabulum) is motionless. Both cylindrical surfaces are motionless in α_3 longitudinal direction. Hence, we have:

$$U_1 = \omega h_1 \quad \text{and} \quad \alpha_1 = \varphi, \quad \alpha_2 = r, \quad \alpha_3 = z. \tag{27}$$

Lubricated is the cylindrical surface region with always monotone generating line $\alpha_3 = z$ inside the intervals: $0 < \varphi < \pi/2$; $-b/2 < z < +b/2$, z – longitudinal coordinate.

Thus, the Lamé coefficients and lubrication region are as follows:

$$h_1 = R, \quad h_2 = 1, \quad h_3 = 1, \quad \Omega = \pi R b/2, \tag{28}$$

where R [m] denotes the radius of the cylindrical bone. Geometrical simulation of elbow cylindrical joint shows Fig. 2.

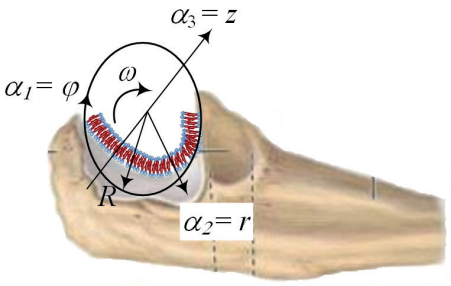

Fig. 2. Geometry of rotational region of cylindrical elbow joint

For the analysed stochastic lubrication of the human hip joint, taking into account the PL bilayer, the following spherical coordinate system seems the most appropriate: $\alpha_1 = \varphi$, $\alpha_2 = r$, $\alpha_3 = \vartheta$. Lamé coefficients for the thin layer of lubricating fluid on a spherical rotational surface with a monotonic generating line are as follows: $h_1 = R\sin\vartheta_1$, $h_2 = 1$, $h_3 = 1$, where R is the radius of the spherical bone head and $\vartheta_1 = \vartheta/R$. We substitute the presented spherical coordinates and the given Lamé coefficients to formulas (14)–(18), (23)–(26). The expected functions of fluid velocity vector components determined by formulas (14), (16), (18) will take the following form: $EX[v_\varphi(\varphi, r, \vartheta)]$, $EX[v_r(\varphi, r, \vartheta)]$, $EX[v_\vartheta(\varphi, r, \vartheta)]$. Expected functions of friction force components $EX(F_{R1})$, $EX(F_{R3})$ represented by formulas (23)–(24) are transformed into $EX(F_{R\varphi})$, $EX(F_{R\vartheta})$. Electric field components M_1, M_3 are replaced by components M_φ, M_ϑ. Auxiliary subordinate functions $A_{\rho i}$ for $i = 1, 2, 3$, represented by formula (17), take the following forms: $A_{\rho\varphi}$, $A_{\rho r}$, $A_{\rho\vartheta}$.

The dimensionless height of the human hip joint gap, limited by nominally smooth spherical surfaces of articular cartilage, deformed by random changes, in accordance with the designation provided in formula (1), can be represented in the following dimensional form [3]:

$$\begin{aligned}\varepsilon_T(\varphi, \vartheta_1, \delta_1) &= \varepsilon_0 \varepsilon_{T1}(\varphi, \vartheta_1, \delta_1) \\ &\equiv \varepsilon_0 \varepsilon_{T1s}(\varphi, \vartheta_1)[1 + \delta_1(\varphi, \vartheta_1)],\end{aligned} \tag{29}$$

where classical gap height $\varepsilon_T(\delta_1 = 0) = \varepsilon_0 \varepsilon_{T1s}(\varphi, \vartheta_1)$ had been derived in papers [3, 24].

The symbol ε_0 means a constant, characteristic, dimensional value of joint gap height. We assume the centre of the spherical bone head to be at $O(0, 0, 0)$. The centre of the spherical surface of the acetabulum is at $O_1(x - \Delta\varepsilon_x, y - \Delta\varepsilon_y, z + \Delta\varepsilon_z)$. Eccentricity has the value of D, see Fig. 3.

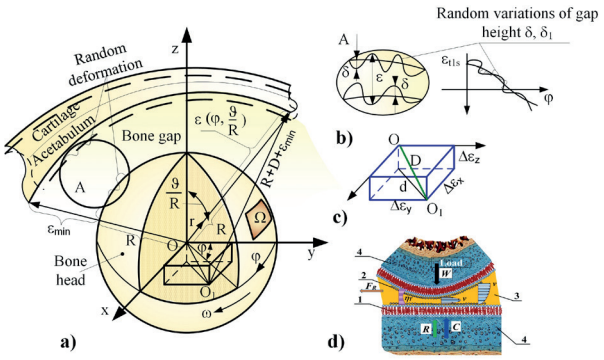

Fig. 3. Gap height for randomly deformed articular cartilage surface: a) joint gap between the femoral head and the acetabulum, b) random changes δ in gap height, c) eccentricity of the centre points of the spherical head and the acetabulum, d) hip joint dynamics, where: W – joint load, C – load-carrying capacity, R – repulsion force, 1 – phospholipid bilayer, 2 – hydrated sodium ions, 3 – synovial fluid, 4 – articular cartilage, η_T – synovial fluid viscosity distribution in the direction of layer thickness

Lubrication area Ω is determined by the following inequalities: $0 < \varphi < \pi$; $\pi R/8 < \vartheta < \pi R/2$, $\vartheta = \vartheta_1 R$.

6. Semi-analytical and experimental estimation of random lubricant parameters

We now present an estimation of the value of the expected functions of random load-carrying capacity and friction forces in the hip joint based on the obtained analytical solutions (Section 4) and stochastic gap height analysis (Section 2) without detailed numerical calculations.

Using probability density function f for corrections δ_1 of the gap height, we determine the expected value, i.e. $EX(\delta_1) = m$, from Formula (2a); from Eq. (3) we calculate standard deviation σ. The equation that enables the estimation of the expected values of gap height, was based on Eqs. (1) and (2b), and has the following form:

$$\begin{aligned}(1 + m - \sigma)\,\varepsilon_T(\delta_1 = 0) \le EX(\varepsilon_T) \le \\ \le (1 + m + \sigma)\,\varepsilon_T(\delta_1 = 0),\end{aligned} \tag{30}$$

where $\varepsilon_T(\delta_1 = 0)$ denotes the gap height without random corrections.

Figure 4 illustrates the influence of stochastic changes in the susceptibility of the multimode boundary areas of the flowed around cartilage surface and gap height on the values of lubrication parameters. The left column of the illustration, a)–d),

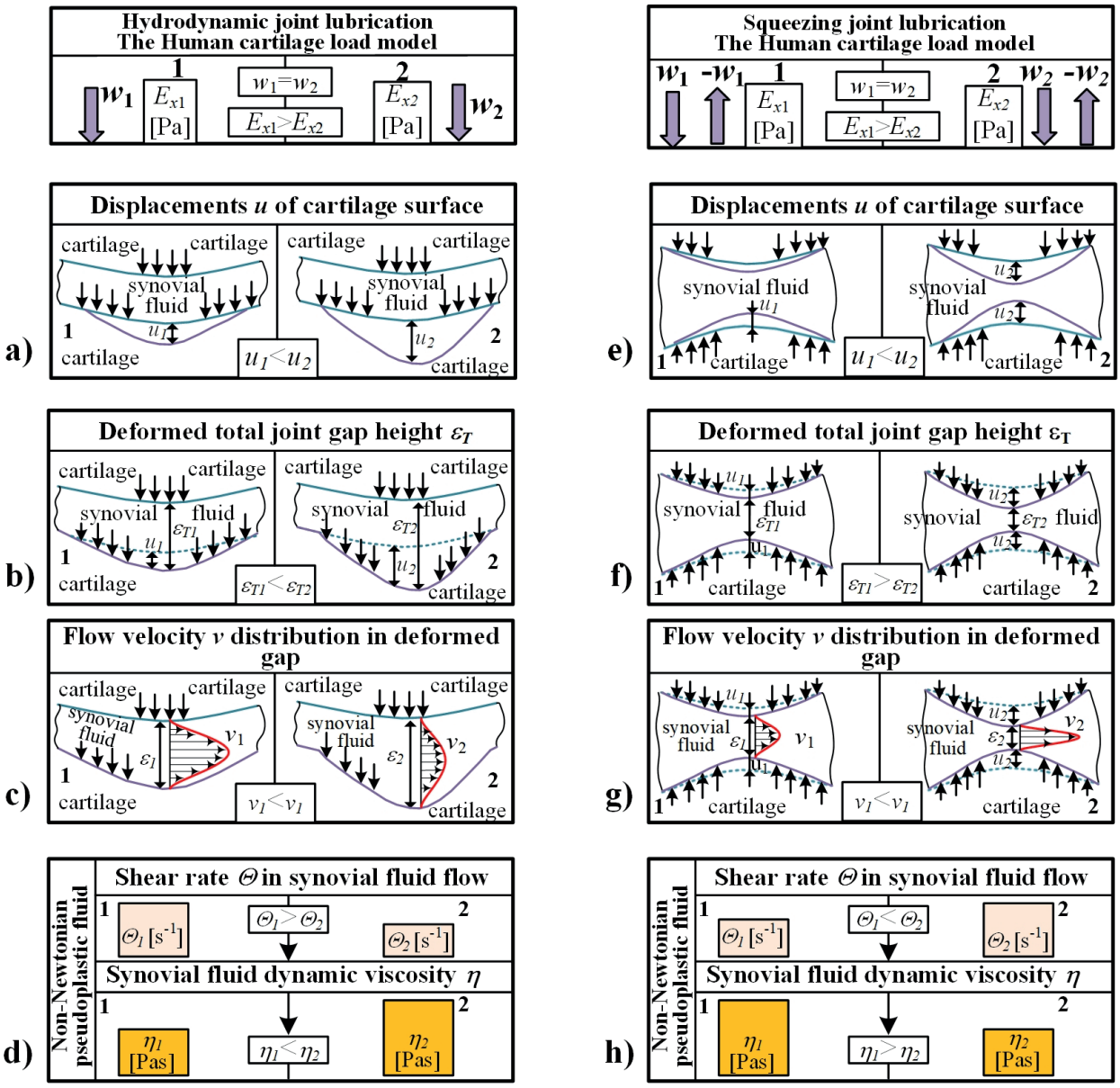

Fig. 4. The stochastic influence of the elasto-hydrodynamic change in the susceptibility of multimode cartilage surface in contact with flowing fluid on its viscosity in a thin gap, for cartilage lubrication by means of classical hydrodynamics on the left (a, b, c, d) and by squeezing out on the right (e, f, g, h), where random changes show: a), e) displacements at the cartilage surface, b), f) decreases and increases in height ε_T of the joint gap, c), g) decreases and increases of synovial fluid flow velocity profile in the gap, d), h) changes in shear rate causing increases and decreases in synovial fluid viscosity on boundary surfaces between susceptibility change $E_{x1} \neq E_{x2}$ of a molecule being flowed around

relates to hydrodynamic lubrication by rotational movement, while the right column of the illustration, e)–h), describes lubrication by squeezing out synovial fluid. Each column of the illustration consists of a left side loaded with force W_1 and a right side loaded with force $W_2 = W_1$. The left side concerns the less susceptible (more durable) superficial layer of articular cartilage with a greater modulus of elasticity and plasticity E_{x1}. The right side concerns the more susceptible (less durable) multimode superficial layer of articular cartilage with a smaller modulus of elasticity and plasticity $E_{x2} < E_{x1}$. Similarly, the effect of viscosity change would be obtained by assuming $W_2 > W_1$ and $E_{x2} = E_{x1}$.

Figure 4 shows that with randomly increasing (decreasing) gap height: Fig. 4b, 4f, synovial fluid flow velocity in the gap decreases (increases): Fig. 4c, 4g. This results in a decrease (increase) in flow shear rate Θ: Fig. 4d, 4h. Since synovial fluid has non-Newtonian properties, an increase (decrease) in shear rate implies a decrease (increase) in dynamic viscosity η_T of synovial fluid, see Fig. 4d, 4h.

For stationary flow of synovial fluid in the joint gap, there is an equal volumetric flow rate in places of narrowing and expansion of gap height ε_T, both in the case of classic hydrodynamic lubrication as well as lubrication by squeezing out. The flow rate, as the product of average flow velocity and flow

surface, implies an increase (decrease) in velocity v, which is inversely proportional to the narrowing (widening) of the gap height shown in Fig. 4a, b, c, e, f, g. Thus, we have the following estimation of the value the expected velocity function:

$$\frac{v(\delta_1=0)}{1+m+\sigma} \le EX(v) \le \frac{v(\delta_1=0)}{1+m-\sigma}, \tag{31}$$

where $v(\delta_1=0)$ denotes the velocity without random corrections of gap height.

The presented implication of viscosity changes illustrated in Fig. 4 is confirmed by formula (9a) defining apparent viscosity η_T. In this formula, an increase (decrease) in velocity v implies a decrease (increase) in the dynamic viscosity of synovial fluid.

Thus, using the expected value of gap height corrections m, and its standard deviation σ and after numerical estimations for expressions (9a) we obtain the following inequalities for the value of the expected viscosity function:

$$\begin{aligned}(1+m-\sigma) \le \frac{EX(\eta_T)}{\eta_T(\delta_1=0)} \le (1+m+\sigma),\\ \eta_T(\delta_1=0) = O\left(\frac{\gamma_{\max}+k\cdot A^{-1}T\cdot \ln L}{\delta_v\cdot v_0}\right),\end{aligned} \tag{32a}$$

where $\eta_T(\delta_1=0)$ denotes the biological liquid viscosity without random corrections of gap height and without susceptibility random changes on the superficial layer of surfaces.

By virtue of Eq. (32a) we calculate the apparent dynamic viscosity for synovial fluid taking into account the following parameter values: $A=10^{-15}$ m^2, $\ln L=-50$, $\gamma=2.5$ mJ/m^2, 0.03 m/s $< v_0 <$ 0.04 m/s, $T=310$ K, $k=1.380649\cdot 10^{-23}$ J/K, $\delta_v=0.2$. Hence: $kA^{-1}T\cdot\ln L=-0.214$ mN/m.

The non-stochastic apparent viscosity has the following value:

$$\begin{aligned}\eta_T(\delta_1=0) &= \frac{\gamma_{\max}+k\cdot A^{-1}T\cdot\ln L}{\delta_v\cdot v_0} = \\ &= \frac{2.5\ \frac{\text{mN}}{\text{m}} - 0.2140\ \frac{\text{mN}}{\text{m}}}{0.20\cdot 0.0368\ \frac{\text{m}}{\text{s}}} = 0.3105\ \text{Pa}\cdot\text{s}.\end{aligned} \tag{32b}$$

Symbols: A, L, γ and k – Boltzmann constant are described in Section 3. It is visible that the boundary surface A between areas of different phospholipid concentrations has the important influence on the bio-fluid viscosity variations.

The derived formula (32a) for the apparent viscosity of biological liquid shows directly that increments of phospholipids concentration on the joint cartilage surface corresponding with the decrements of the value 0.6 to the value 0.2 of the dimensionless coefficient δ_v, implies the increments of apparent dynamic viscosity. The experimental studies [1, 8] confirm this phospholipid feature.

The derived formula (32a) for the apparent viscosity of biological liquid shows directly that decrements of the flow velocity v_0 of the biological liquid in the joint gap during the lubrication increases apparent dynamic viscosity of the biological liquid.

After fundamental laws of the fluid mechanics it follows, that the velocity distribution of the liquid flow in the conduit gap has parabolic shape, whereas the lowest values of velocity are located on the boundary surfaces of the gap which are restricted the liquid layer. Experimental studies [2, 6] confirm, that the highest values of the dynamic viscosity of the lubricated biological liquid are occurring on the laminar boundary layer of the cartilage which is flowed around by the biological liquid.

The sequence of drawings 4a–h shows that smaller gap height implies lower viscosity of non-Newtonian liquid. This fact applies to the fluid for both hydrodynamic classic lubrication (left column) as well as (right column) joint surface lubrication by squeezing out (right column).

The expected function of hydrodynamic pressure p determined from differential equation (19), with the simultaneous use of inequalities (31), (32), enables the estimation of its value in the following interval:

$$\begin{aligned}\frac{1+m-\sigma}{(1+m+\sigma)^2} \le \frac{EX(p)}{p(\delta_1=0)} \le \frac{1+m+\sigma}{(1+m-\sigma)^2},\\ p(\delta_1=0) \equiv O\left(\frac{R^2\omega\eta_T(\delta_1=0)}{\varepsilon_T^2(\delta_1=0)}\right).\end{aligned} \tag{33}$$

The expected values of load-carrying capacity $C=pS$ for pressure p within range (33), determined from formula (25) on cartilage surface $S=d\alpha_1 d\alpha_3$ are limited in the following interval:

$$\begin{aligned}\frac{1+m-\sigma}{(1+m+\sigma)^2} \le \frac{EX(C)}{C(\delta_1=0)} \le \frac{1+m+\sigma}{(1+m-\sigma)^2},\\ C(\delta_1=0) \equiv O\left(\frac{R^2S\omega\eta_T(\delta_1=0)}{\varepsilon_T^2(\delta_1=0)}\right).\end{aligned} \tag{34}$$

The expected function of friction forces F_R with the simultaneous use of inequalities (31), (32), enables the estimation of its value in the following interval:

$$\begin{aligned}\frac{1+m-\sigma}{1+m+\sigma} \le \frac{EX(F_R)}{F_R(\delta_1=0)} \le \frac{1+m+\sigma}{1+m-\sigma},\\ F_R(\delta_1=0) \equiv O\left(\frac{SR\omega\eta_T(\delta_1=0)}{\varepsilon_T(\delta_1=0)}\right).\end{aligned} \tag{35}$$

The expected function of the coefficient of friction $\mu=F_R/C$, expressed by formula (26), with the simultaneous use of inequalities (34), (35), enables the estimation of its value in the following interval:

$$\begin{aligned}1+m-\sigma \le \frac{EX(\mu=F_R/C)}{\mu(\delta_1=0)} \le 1+m+\sigma,\\ \mu(\delta_1=0) \equiv O\left(\frac{\varepsilon_T(\delta_1=0)}{R}\right).\end{aligned} \tag{36}$$

7. The method of experimental determination for the gap height random density function

The intervals of analytical bio-tribological parameters (30)–(36) will now be considered for specific results of experimental studies. Experimental studies [1] and [2] regarding the measurement of hip joint gap height with radial clearance ε_0 from 2 μm to 10 μm prove that the dimensionless random variable of corrections for gap height, marked with the symbol δ_1, is most often manifested by two characteristic types of probability density functions. These are symmetrical and anti-symmetrical functions. Symmetrical density functions of correction parameters occur much less frequently than anti-symmetrical functions (about 12 times in 100 measurements with a probability of $P_s = 0.12$). They are characterized by a symmetrical distribution of random probability changes in terms of gap height increases and decreases. The probabilities of random increases in joint height gap are equal to the probabilities of random decreases. Symmetrical probability density function f_S is described by the following equations:

$$f_S(\delta_1) \equiv \begin{cases} 1+\delta_1 & \text{for } -1 \le \delta_1 \le 0, \\ 1-\delta_1 & \text{for } 0 \le \delta_1 \le 1, \\ 0 & \text{for } |\delta_1| > 1. \end{cases} \tag{37}$$

Among the frequently occurring unsymmetrical correction parameter density functions describing increases and decreases in gap height, we generally have two types of functions. The first type (38a, b) concerns function f_N, where the probabilities of random gap height increases dominate over the probabilities of random gap height decreases. The second type (38c, d) concerns function f_n, where the probabilities of random gap height decreases dominate over the probabilities of random gap height increases. The two cases a) and b) for anti-symmetrical probability density distribution functions f_N, each one of them occurring 22 times in 100 measurements with probability $P_N = 0.22$, are described by Eqs. (38a, b).

$$f_N(\delta_1) \equiv \begin{cases} \frac{1}{2}\delta_1 + \frac{1}{2} & \text{for } -1 \le \delta_1 \le -\frac{1}{2}, \\ \frac{3}{2}\delta_1 + 1 & \text{for } -\frac{1}{2} \le \delta_1 \le 0, \\ -\frac{1}{2}\delta_1 + 1 & \text{for } 0 \le \delta_1 \le \frac{1}{2}, \\ -\frac{3}{2}\delta_1 + \frac{3}{2} & \text{for } \frac{1}{2} \le \delta_1 \le +1, \\ 0 & \text{for } |\delta_1| > 1; \end{cases} \tag{38a}$$

$$f_N(\delta_1) \equiv \begin{cases} \frac{1}{3}\delta_1 + \frac{1}{3} & \text{for } -1 \le \delta_1 \le -\frac{1}{4}, \\ 3\delta_1 + 1 & \text{for } -\frac{1}{4} \le \delta_1 \le 0, \\ -\frac{1}{3}\delta_1 + 1 & \text{for } 0 \le \delta_1 \le \frac{3}{4}, \\ -3\delta_1 + 3 & \text{for } \frac{3}{4} \le \delta_1 \le +1, \\ 0 & \text{for } |\delta_1| > 1. \end{cases} \tag{38b}$$

The two cases c) and d) for anti-symmetrical probability density distribution functions f_n, each one of them occurring 22 times in 100 measurements with probability $P_n = 0.22$, are described by Eqs. (38c, d).

$$f_n(\delta_1) \equiv \begin{cases} 3\delta_1 + 3 & \text{for } -1 \le \delta_1 \le -\frac{3}{4}, \\ \frac{1}{3}\delta_1 + 1 & \text{for } -\frac{3}{4} \le \delta_1 \le 0, \\ -3\delta_1 + 1 & \text{for } 0 \le \delta_1 \le \frac{1}{4}, \\ -\frac{1}{3}\delta_1 + \frac{1}{3} & \text{for } \frac{1}{4} \le \delta_1 \le +1, \\ 0 & \text{for } |\delta_1| > 1; \end{cases} \tag{38c}$$

$$f_n(\delta_1) \equiv \begin{cases} \frac{3}{2}\delta_1 + \frac{3}{2} & \text{for } -1 \le \delta_1 \le -\frac{1}{2}, \\ \frac{1}{2}\delta_1 + 1 & \text{for } -\frac{1}{2} \le \delta_1 \le 0, \\ -\frac{3}{2}\delta_1 + 1 & \text{for } 0 \le \delta_1 \le \frac{1}{2}, \\ -\frac{1}{2}\delta_1 + \frac{1}{2} & \text{for } \frac{1}{2} \le \delta_1 \le +1, \\ 0 & \text{for } |\delta_1| > 1. \end{cases} \tag{38d}$$

Symmetrical distribution (37) of density function f_s is shown in Fig. 5. Unsymmetrical distributions (38a–d) for function f_N, f_n are illustrated in Fig. 6. The measurement multiplicity shown in Fig. 5, Fig. 6a–d, equal to $12+2\times22+2\times22=100$, creates a probabilistic complete system of events.

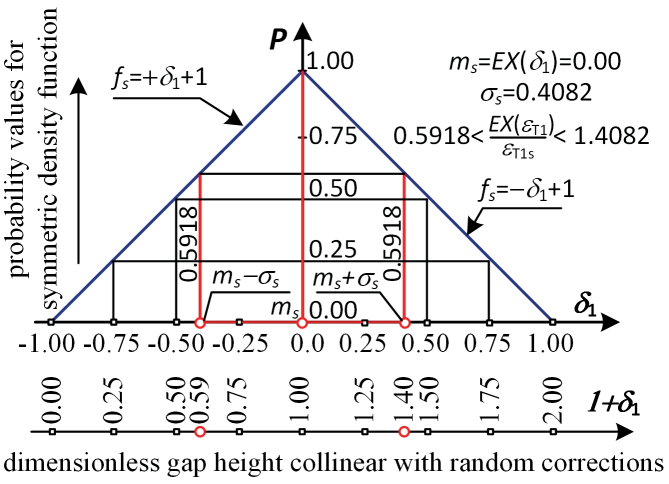

Fig. 5. Symmetrical probability density function f_S according to formula (37), with a vertical axis of probability P, where the upper horizontal axis gives dimensionless values of the random variable of corrections δ_1 of increases and decreases in joint gap height, the lower horizontal axis indicates the height of the entire gap $1+\delta_1$

Unsymmetrical f_N, f_n distributions of probability density functions (38a, b), (38c, d) together with the determined expected values and standard deviations are presented in Fig. 6a–d.

For symmetrical function (37), expected value $m_s = 0$ for the random variable of gap height corrections was determined from

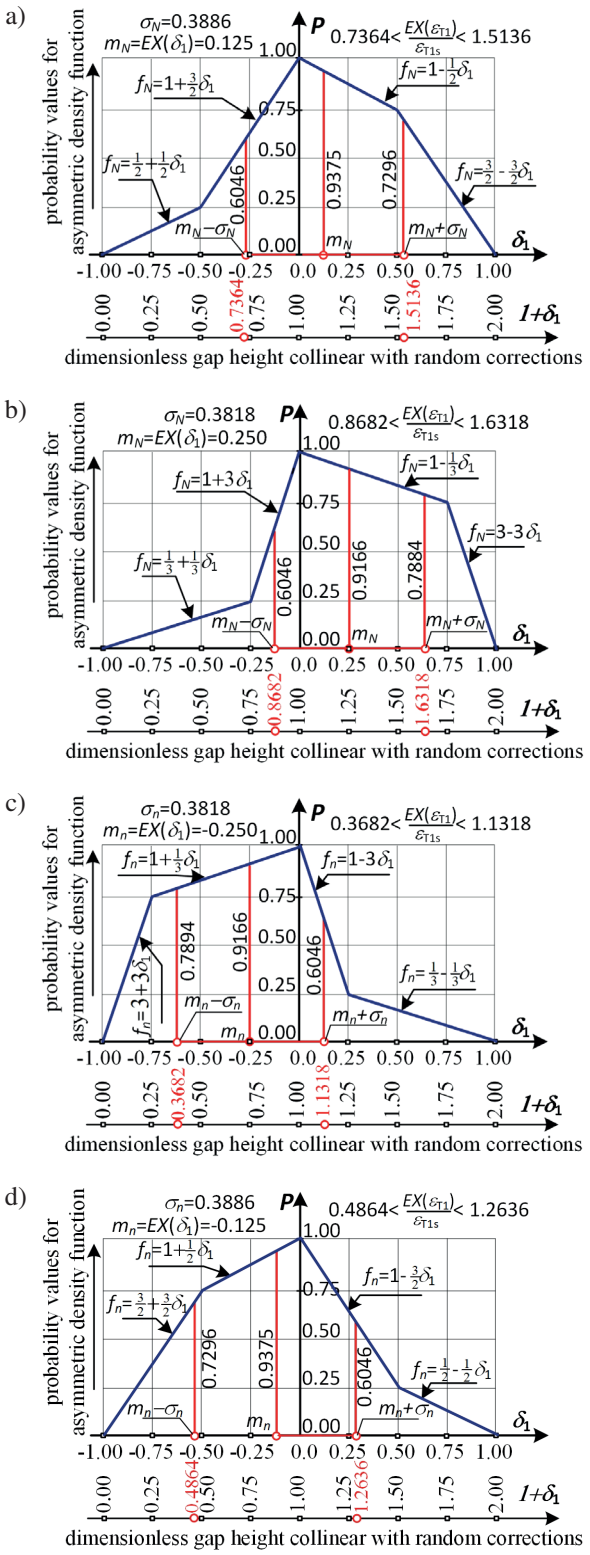

Fig. 6. Anti-symmetrical probability density functions: a), b) according to formulas (38a,b) for f_N dominance of random increases over decreases of joint gap height, c), d) according to formula (38c, d) for f_n dominance of random decreases over random increases of joint gap height; where the vertical axis indicates probabilities P, the upper horizontal axis gives dimensionless values of the random variable of increase and decrease corrections of joint gap height δ_1, the lower horizontal axis indicates the heights of the entire gap $1+\delta_1$

formula (2). The standard deviation determined from formula (3) gives the following value: $\sigma_s = 0.4082$. The standard deviation interval is:

$$(m_s - \sigma_s, m_s + \sigma_s) = (-0.4082, +0.4082). \tag{39}$$

This interval was superimposed onto Fig. 5 on upper horizontal axis δ_1. In this interval, due to random changes for the measurements conducted, the random expected value of increases and decreases in gap height may change its location. The changes are assigned a change value of the entire gap, read from lower horizontal axis $1+\delta_1$, where dimensionless gap height equal to 1 is assigned to value correction $\delta_1 = 0$ on the upper horizontal axis. Thus, we obtain range of variations of the expected function values of the dimensional height. The height of the entire gap may decrease or increase. Such changes in gap height occur with a probability from $P_s = 0.5918$ to $P_s = 1.0000$, indicated on the vertical axis Fig. 5.

For non-symmetrical functions (38a–d), the following expected values for the random variable of gap height corrections were determined from formula (2): $m_N = +0.125$; $m_N = +0.250$, $m_n = -0.250$; $m_n = -0.125$. The standard deviations of the random variable of corrections determined from formula (3) give the following values: $\sigma_N = 0.3886$; $\sigma_N = 0.3818$; $\sigma_n = 0.3818$; $\sigma_n = 0.3886$. The standard deviation intervals of the random variable of corrections $(m_N - \sigma_N,\ m_N + \sigma_N)$, $(m_n - \sigma_n,\ m_n + \sigma_n)$, superimposed onto Fig. 6a–d on axis δ_1, are as follows:

$$\begin{aligned}&(-0.2636,\ +0.5136);\ (-0.1318,\ +0.6318);\\ &(-0.6318,\ +0.1318);\ (-0.5136,\ +0.2636).\end{aligned} \tag{40}$$

In this interval, due to random changes, the random expected value of increases and decreases in gap height may change its location. The changes are assigned a change value of the entire gap, read on collinear second horizontal axis $1+\delta_1$. Thus, we obtain range of variations of the expected function values of the dimensional height.

Changes in gap height occur successively with probabilities from $P_N = 0.6046$ through $P_N = 0.7884$; $P_N = 0.9166$ to $P_N = 1.0000$ indicated on the vertical axis in Fig. 6a, b, similarly with the P_n probabilities in Fig. 6c, d.

Based on the conclusions from the studies illustrated in Figs. 5, 6a–d, the following forms of expected values of the lower and upper limits of the standard deviation interval of joint gap height are derived:

$$\varepsilon_T(1+m-\sigma) = \varepsilon_T \sum_{i=s,n,N} P_i(1+m_i-\sigma_i) = 0.6120\varepsilon_T\,, \tag{41a}$$

$$\varepsilon_T(1+m+\sigma) = \varepsilon_T \sum_{i=s,n,N} P_i(1+m_i+\sigma_i) = 1.3879\varepsilon_T\,. \tag{41b}$$

8. Experimental results

Based on the conducted calculations (41) and inequalities (30), (31), (32), the value of the expected function of joint gap height, the speed of synovial fluid, and its viscosity change together

with probability: $0.6708 \leq P \leq 1.0000$ in the following value intervals:

$$0.6120\varepsilon_T(\delta_1=0) = (1+m-\sigma)\varepsilon_T(\delta_1=0) \leq EX(\varepsilon_T) \leq \leq (1+m+\sigma)\varepsilon_T(\delta_1=0) = 1.3879\varepsilon_T(\delta_1=0), \quad (42a)$$

$$0.7205v(\delta_1=0) = (1+m+\sigma)^{-1}v(\delta_1=0) \leq EX(v) \leq \leq (1+m-\sigma)^{-1}v(\delta_1=0) = 1.6339v(\delta_1=0), \quad (42b)$$

$$0.6120\eta_T(\delta_1=0) = (1+m-\sigma)\eta_T(\delta_1=0) \leq EX(\eta_T) \leq \leq (1+m+\sigma)\eta_T(\delta_1=0) = 1.3879\eta_T(\delta_1=0). \quad (42c)$$

We assume the following designations for dimensionless ratios (quotients) of stochastic functions determined from the system of Eqs. (4)–(9) including operator EX, to non-stochastic functions (excluding operator EX) for pressure, load-carrying capacity, frictional forces, and coefficients of friction:

$$\xi_p \equiv \frac{EX(p)}{p(\delta_1=0)}, \qquad \xi_C \equiv \frac{EX(C)}{C(\delta_1=0)}, \qquad \xi_F \equiv \frac{EX(F_R)}{F_R(\delta_1=0)}, \qquad \xi_\mu \equiv \frac{EX(\mu)}{\mu(\delta_1=0)}. \quad (42d)$$

The denominators of fractions (42d) are obtained by assuming a gap without stochastic decrease or increase. We obtain the fraction nominators by assuming stochastic changes in the range of intervals (42a–c). We analyse the example of experimentally determined probability density functions shown in Figs. 5 and 6. We use estimations (33)–(36) and take into account the expected values of the upper and lower limits of standard deviations (42a–c).

We assume coefficients α and β depending on radial clearances (characteristic values of gap height ε_0) and the dimensionless range of stochastic changes represented by formulas (42a–c). Then the dimensionless stochastic changes of lubrication parameters presented as quotients of function are in the following intervals:

$$\xi_{p\min} = 0.3177\alpha_p \leq \xi_p \leq 3.7055\beta_p = \xi_{p\max}, \quad (43a)$$

$$\xi_{C\min} = 0.3177\alpha_C \leq \xi_C \leq 3.7055\beta_C = \xi_{C\max}, \quad (43b)$$

$$\xi_{F\min} = 0.4409\alpha_F \leq \xi_F \leq 2.2678\beta_F = \xi_{F\max}, \quad (43c)$$

$$\xi_{\mu\min} = 0.6120\alpha_\mu \leq \xi_\mu \leq 1.3879\beta_\mu = \xi_{\mu\max}, \quad (43d)$$

Dimensionless values $\xi_{\min}$, $\xi_{\max}$ appearing in formulas (43) are obtained from fractions (42d), in which we calculate denominator values assuming a gap without stochastic decreases or increases. We calculate fraction nominators $\xi_{\min}$ by assuming the stochastic changes (42a–c) for which the fraction value is the lowest. We calculate fraction nominators $\xi_{\max}$ by assuming the stochastic changes (42a–c) for which the fraction value is the highest.

9. Numerical calculations

Numerical solutions mainly concern stochastic and non-stochastic (excluding operator EX) non-linear partial differential equation (19), determining two-dimensional hydrodynamic pressure p, and Eq. (20), describing three-dimensional temperature distribution T. These equations converted to spherical coordinates (φ, r, ϑ) are mutually coupled through three-dimensional dynamic viscosity function η_T represented by formula (9), variable in the direction of gap height and dependent on temperature. The coupling of the equations consists in the simultaneous dependence of pressure on temperature and temperature on pressure.

Numerical integration of coupled equations was carried out using the method of convergent sequence of successive approximate solutions. In the first step of approximation, a constant dimensionless viscosity equal to one was assumed. Hydrodynamic pressure for constant viscosity was determined, followed by temperature distribution. In the second step of calculations, the obtained pressure and temperature values were used to determine the variable 3D viscosity value. Hydrodynamic pressure and temperature distribution were calculated using the obtained variable viscosity. In the subsequent steps of calculations, the described procedure was repeated until the obtained sequence of pressure and temperature functions was convergent with the boundary function of pressure and temperature. The convergence of such a sequence to the boundary function of pressure and temperature, regardless of the value of the assumed constant viscosity at the beginning of the calculation process, indicates that the solution of the coupled equation system was obtained correctly. The calculations were carried out using the finite difference method, using our own numerical procedures and professional Mathcad 15 software. After numerically calculating pressure and temperature (successive approximations and differential method), frictional force was determined from formulas (23), (24), and then load-carrying capacity C and coefficient of friction μ, based on formulas (26), (36).

Based on the numerical calculations of the semi-analytical solutions of differential equations (19), (20), (23)–(36), the values of coefficients α and β as well as the maximum and minimum indices $\xi_{\max}$, $\xi_{\min}$ were obtained, listed in Table 1 as quotients (43) of stochastic values to non-stochastic values for pressure, load carrying capacity, frictional forces, coefficients of friction.

Fig. 7a–c presents changes in dimensional values of load-carrying capacity and frictional forces as well as changes in the dimensionless coefficient of friction for stochastic changes in gap height versus the characteristic dimensional gap height. The results were obtained based on the numerical solution of the stochastic system of partial differential equations (19), (20) for spherical coordinates.

Numerical calculations took into account the influence of phospholipid concentration on the surface of articular cartilage ($A = 10^{-15}$ m^2); electric field ($M_i = 0$, $M_T = 0$) was omitted. For pressure and temperature, boundary conditions (21), (22) and density functions of variable random joint gap height ε_T, described by formulas (37), (38), were assumed. In addition, the following was assumed: $\ln L = -50$, characteristic value of synovial fluid flow velocity in the joint gap $0.03\ \mathrm{m/s} < \mathrm{v}_0 < 0.0\ 4\mathrm{m/s}$, interfacial energy $0.1\ \mathrm{mN/m} < \gamma < 4\ \mathrm{mN/m}$, coefficient of collagen fibre concentration $0.2 < \delta_v < 0.6$, character-

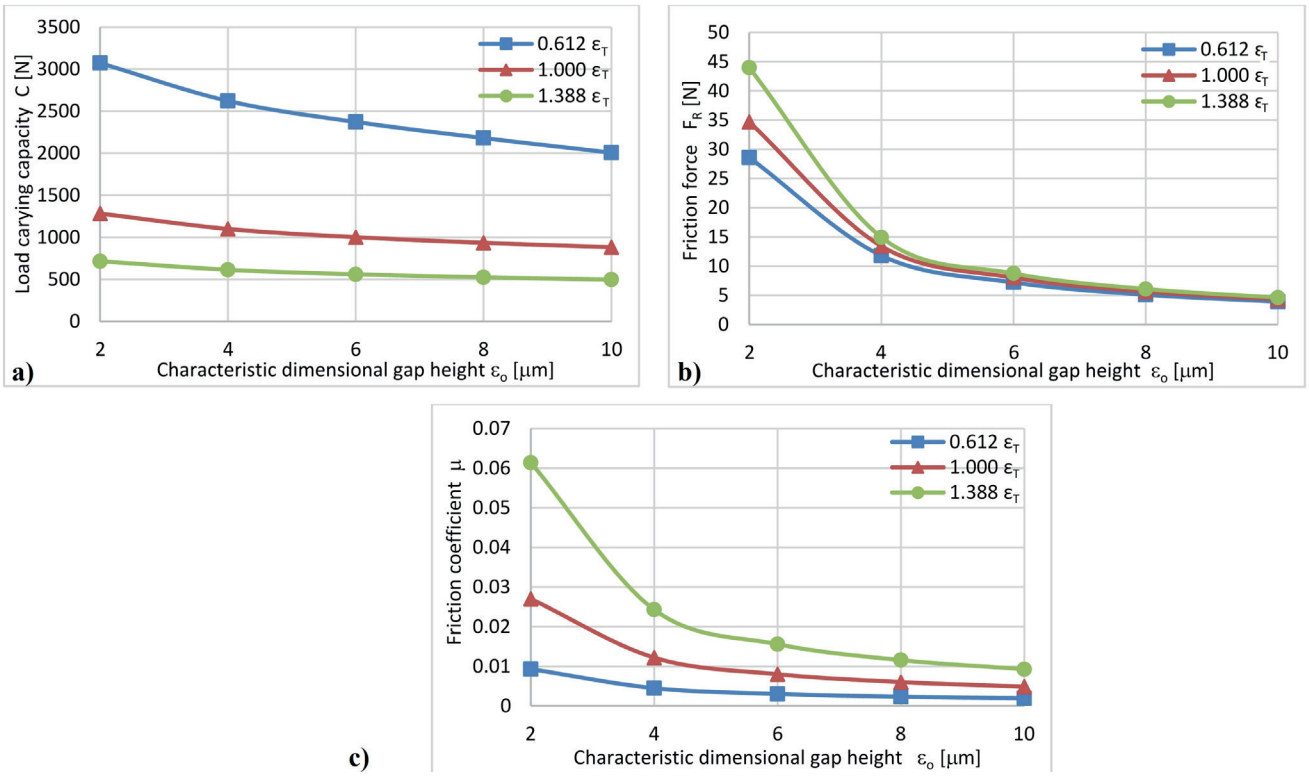

Fig. 7. Load-carrying capacity a) frictional forces; b) coefficients of friction; c) for stochastic changes in gap height $0.612 \cdot \varepsilon_T$ and $1.388 \cdot \varepsilon_T$, and in the absence of stochastic changes $1.000 \cdot \varepsilon_T$ for a hip with radial clearance ε_0 equal to 2 μm, 4 μm, 6 μm, 8 μm, 10 μm

Table 1
Probabilistic and numerical parameters for stochastic changes in gap height in the form: $0.6120 < EX(\varepsilon_T)/\varepsilon_T(\delta_1 = 0) < 1.3879$ for a hip with radial clearance ε_0 equal to 2 μm, 4 μm, 6 μm, 8 μm, 10 μm

ξ, α, β	ε_0				
	2 μm	4 μm	6 μm	8 μm	10 μm
$\xi_{p\min}$	0.558664	0.560021	0.561597	0.563306	0.566334
$\xi_{p\max}$	2.387635	2.372290	2.352564	2.314966	2.259481
α_p	1.758464	1.762735	1.767696	1.773075	1.782606
β_p	0.644349	0.640207	0.634884	0.624738	0.609764
$\xi_{C\min}$	0.557866	0.558636	0.559780	0.561197	0.563589
$\xi_{C\max}$	2.393302	2.383636	2.367265	2.331374	2.272007
α_C	1.755952	1.758374	1.761976	1.766437	1.773066
β_C	0.645878	0.643269	0.638851	0.629149	0.613144
$\xi_{F\min}$	0.824445	0.879285	0.897883	0.905707	0.909492
$\xi_{F\max}$	1.267801	1.113264	1.089166	1.077987	1.071942
α_F	1.869914	1.994295	2.036478	2.054224	2.062807
β_F	0.559044	0.490900	0,480274	0.475345	0.472679
$\xi_{\mu\min}$	0.344412	0.369016	0.379336	0.388493	0.400410
$\xi_{\mu\max}$	2.272391	1.992623	1.945346	1.920080	1.902154
α_μ	0.562764	0.602968	0.619830	0.634792	0.654265
β_μ	1.637287	1.435711	1.401647	1.383442	1.370527

istic value of synovial fluid dynamic viscosity $\eta_0 = 0.300$ Pas, radius of the sphere of the femoral head $R = 0.0265$ m, characteristic value of ambient temperature $T_0 = 310$ K.

The following detailed conclusions result from the conducted experimental tests enabling the determination of probability density functions (37), (38), illustrated in Figs. 5 and 6, and from the values obtained from numerical calculations given in Table 1:

- Stochastic interactions can cause decreases to 58.8% or increases to 239% of the 100% value of pressure p, load-carrying capacity C obtained for $\delta_1 = 0$ in the joint gap, without taking into account random changes in gap height, synovial fluid viscosity, and temperature, i.e. when: $\varepsilon_T(\delta_1 = 0)$, $\eta_T(\delta_1 = 0)$, $T(\delta_1 = 0)$. This conclusion results from inequality (33), (34), from formula (19), (25), determining expected value of pressure, load-carrying capacity $EX(p)$, $EX(C)$, and from estimations (43a, b).
- Random changes can cause decreases of up to 82.4% and increases of up to 126.7% of the 100% value of friction force F_R for $\delta_1 = 0$ in the joint gap, obtained without taking into account random changes in gap height, synovial fluid viscosity, and temperature. This conclusion results from inequalities (35), (43c) and from stochastic equations (23), (24), determining expected values of friction force vector components $EX(F_{R1})$, $EX(F_{R3})$.
- Random changes can cause changes from 34.4% to 227% in coefficient of friction μ for $\delta_1 = 0$ with a value of 100% in the joint gap, obtained without taking into account ran-

dom changes in gap height, synovial fluid viscosity, load-carrying capacity, or friction. The validity of this conclusion results from inequalities (36), (43d), and from formula (26), determining the expected value of the coefficient of friction.

The relatively wide intervals of changes in expected values (43a–d) for lubrication parameters result from the nature of the numerous experimental tests carried out and the measured values of probability density functions (37), (38).

10. Final conclusions

10.1. This paper had proved the following main results, which to day have not been discovered in the contemporary domain presenting a few papers of random lubrication theory for biological joint co-operating multimode surfaces coated with phospholipids bilayer:

10.1.1. The random variation of bio-liquid dynamic viscosity across the very thin lubricating bio-liquid layer and the random variations of the flexibility and susceptibility of the joint multimode cartilage superficial layer coated with the phospholipid's bilayer, imply on the about from 10 to 15 percent changes of the spherical joint load carrying capacity.

10.1.2. The 10 percentage increment of the different multimode boundary areas of phospholipid concentration, causes average 15 percentage increments of the apparent dynamic viscosity of biological liquid.

Abovementioned results had been confirmed in analytical and numerical way contained in theoretical considerations as well as by the experimental measurements data manifested in this paper during the elaboration of the many probability density functions for various human joints gap height restricted by the surfaces coated with the phospholipid bilayer.

10.2. Load carrying capacity, friction forces, friction coefficient in the spherical joint are decreasing if radial clearance increases (see Fig. 7):

10.2.1. The joint capacity obtained without random changes of gap height is about 66 percent lower than the capacity for minimum random gap height and is about 30 percent higher than the capacity for maximum random gap height.

10.2.2. Friction forces determined in joint without random changes of gap height is about 12% lower than the friction forces for maximum random gap height and is about 10% higher than the friction forces for minimum random gap height.

10.2.3. Friction coefficient obtained in human joint without random changes of gap height is about 70% lower than the friction coefficient for maximum random gap height and is average 50% higher than the friction coefficient for minimum random gap height.

Abovementioned results had been confirmed in numerical calculations of analytical solutions of random hydrodynamic equations. Obtained numerical values of capacities, friction forces and friction coefficients had been compared with the experimental values of mentioned respective quantities performed in literature [1, 6, 8] where two kinds of phospholipids namely Phosphatidylcholine (PC) and Phosphatidylserine (PS) had been considered and taken into account. The differences between numerical values of capacity, friction forces and friction coefficients obtained in this paper and mentioned respective measured values [1,6,8] attain values in interval from about 5 to 8 percent.

10.3. Random changes in gap height (42a) show the possibility of a decrease in joint gap height of 38.80% and an increase in gap height of 38.79% compared to the gap height determined by formula (29) without random changes for $\delta_1 = 0$. This conclusion results from the conducted research in the case of the considered example of the density function shown in Figs. 5 and 6.

10.4. The density functions shown in Figs. 5 and 6, inequality (31), and solutions (14), (16) for $EX(v)$ imply stochastic estimations (42b) showing a 28% decrease and a 63.39% increase in the value of synovial fluid flow velocity v in the joint gap, compared to the velocity obtained without taking into account random changes in gap height $\delta_1 = 0$.

10.5. Stochastic interactions cause a decrease of 38.0% or an increase of 38.79% in the value of apparent dynamic viscosity of synovial fluid η_T in the joint gap compared to the viscosity for $\delta_1 = 0$, occurring without taking into account random changes in gap height and random changes in synovial fluid flow velocity $v(\delta_1 = 0)$ and temperature $T(\delta_1 = 0)$. This conclusion results from the experimentally determined density functions, from inequalities (32a), (42c), and from formula (9a) determining expected viscosity value $EX(\eta_T)$.

11. Discussion

We analyse the flow of synovial fluid with non-Newtonian properties in a human joint gap between two isotonic surfaces of articular cartilage susceptible to deformations caused by, among others, random changes in surface roughness geometry, stochastic loading of the joint, as well as genetic and volumetric growth of living articular cartilage tissue. The concept of iso-osmosis or iso-tonicity defines layers of biological bodies remaining in osmotic balance with respect to each other.

Isotonic, impermeable biological membranes include, among others, lipid bilayers, which eliminate flow across the layer. The exception may be nanometre channels transporting certain types of liquid.

For the analysed case, this work demonstrated the influence of the physical properties of articular cartilage and gap height on the viscosity of synovial fluid in the area of the boundary layer of the surface flowed around and illustrated it in Fig. 4. According to the authors, the influence of the physical properties of flowed around biological surfaces on the viscosity of the fluid in the boundary layer will be even more visible in lamellar flows, where gap height reaches a value of about 2–3 nm, i.e., the order of the thickness of the phospholipid membrane. Research of random changes in gap height and synovial fluid

viscosity enabled the determination of the interval of random changes in hydrodynamic pressure, frictional forces, and coefficients of friction. Based on the general solutions provided in this paper for each experimental study and the obtained probability density functions, we obtain large or small intervals of estimations for the expected values of bio-tribological parameters. For example, a small interval of changes in expected values, seemingly favourable, but with low probabilities of occurrence, is much less useful than a large interval of changes in expected values of a given parameter with high and low probabilities of occurrence, enabling the assignment of the expected value to the highest possible probabilities of occurrence.

Appendix

We assume an arbitrary, and unsteady, isothermal, incompressible flow of viscoelastic biological liquid in an electro-magnetic field. The abovementioned equations are in the following forms, namely, the equation of motion [22, 23]:

$$\mathrm{Div}\,\boldsymbol{S}+\mu_m(\boldsymbol{N}\boldsymbol{\nabla})\boldsymbol{H}+\boldsymbol{J}\times\boldsymbol{B}+\rho_e\boldsymbol{E}=\rho\,\mathrm{d}\boldsymbol{v}/\mathrm{d}t, \tag{44}$$

the continuity equation:

$$\mathrm{div}(\boldsymbol{v})=0, \tag{45}$$

the reduced Maxwell equation:

$$\nabla^2\boldsymbol{H}\equiv\mu_m\mu_e\frac{\partial^2\boldsymbol{H}}{\partial t^2}, \qquad \boldsymbol{J}=\sigma_e\boldsymbol{E}, \tag{46}$$

the conservation of energy equation:

$$\begin{aligned}\mathrm{div}(\kappa\,\mathrm{grad}\,T)+\Phi_F-\mu_m T\,\boldsymbol{\Xi}(\boldsymbol{v}\nabla)\boldsymbol{H}=0,\\ \Phi_F\equiv\mathrm{div}(\boldsymbol{v}\,\boldsymbol{S})-\boldsymbol{v}\mathrm{Div}\,\boldsymbol{S},\end{aligned} \tag{47}$$

the Young-Kelvin-Laplace equation:

$$\begin{aligned}\gamma=\gamma_{\max}+2sR_gT\ln\left(\sqrt{\frac{K_a}{K_b}}+1\right)\\ -sR_gT\ln\left[\left(\frac{K_a}{a_H^+}+1\right)\left(\frac{a_H^+}{K_b}+1\right)\right],\end{aligned} \tag{48}$$

where: $\boldsymbol{S}$ [Pa] – the stress tensor in biological fluid, $\boldsymbol{E}$ [V/m] – electric intensity vector, $\boldsymbol{J}$ [A/m^2] – electric current density vector, $\boldsymbol{B}$ [T = kg/s^{2}A] – magnetic induction vector in biofluid, $\boldsymbol{v}$ [m/s] – biological fluid velocity vector, $\boldsymbol{H}$ [A/m] – the magnetic intensity vector with components (H_1, H_2, H_3), $\boldsymbol{N}$ [A/m] – the magnetization vector with components (N_1, N_2, N_3), σ_e [S/m] – electrical conductivity of phospholipids bilayer, μ_e [s^{4}A^{2}m^{-3}kg^{-1}] – the electric permeability coefficient of biological fluid, μ_m [mkgs^{-2}A^{-2}] – the magnetic permeability coefficient of biological fluid, κ [W/mK] – thermal conductivity coefficient for biological fluid, Φ_F [W/m^3] – dissipation of energy, Ξ [A/mK] – the first derivative of the magnetization vector with respect to temperature, T [K] – temperature, ρ_e [C/m^3 = As/m^3] – electric space charge in biological fluid, R_g – gas constant (8.3144598 J/K·mol), $s=(\mathrm{N_A}\cdot\mathrm{A})^{-1}$ [mol/m^2] – concentration of phospholipid particles, γ [mJ/m^2 =N/m] – interfacial energy, $\gamma_{\max}$ is the maximum interfacial energy of the lipid membrane whereas 0.1 mN/m $<\gamma_{\max}<$ 4 mN/m, K_a [J] – acid equilibrium constant (denotes how much energy is needed to stretch the bilayer), K_b [J] – base equilibrium constant (denotes how much energy is needed to bend or flex the bilayer), a_H [J] – protons energy activity, A [m^2] – the region of areas of different phospholipids molecules concentration, $\mathrm{N_A}=6.024\cdot10^{23}$ – Avogadro number, ρ [kg/m^3] – biological fluid density. Due to the presence of the phospholipids bi-layers on the cartilage or superficial layer surface and the presence of lipo-somes, micelles, macromolecules and lamellar aggregates in biological fluid, this liquid has non-Newtonian, especially pseudo-plastic properties.

For the synovial fluid, the relationship between stress tensor $\boldsymbol{S}$ and displacement velocity tensor $2\boldsymbol{T}_d=\Theta$, i.e., constitutive equations, are accepted in the following form [23]:

$$\boldsymbol{S}=-p\boldsymbol{\delta}+\eta_T\boldsymbol{\Theta}, \tag{49}$$

whereas unit tensor $\boldsymbol{\delta}$, strain tensor $\boldsymbol{\Theta}$ have the following components: δ_{ij}, Θ_{ij}. We denote: δ_{ij} – Kronecker Delta, p [Pa] – pressure, Θ_{ij} [s^{-1}] – shear rate components.

For non-Newtonian synovial fluid with the model of modified power law, whereas constitutive dependencies for apparent viscosity η_T [Pas] have the following form:

$$\begin{aligned}\eta_T=2^{n-1}m(n)\left|\frac{1}{2}I_1^2(\Theta)-I_2(\Theta)\right|^{\frac{n-1}{2}},\\ I_1(\Theta)=\Theta_{kk}, \qquad I_2(\Theta)=\frac{1}{2}e_{ijk}e_{imn}\Theta_{jm}\Theta_{kn},\end{aligned} \tag{50}$$

where: $I_1(\Theta)$ [s^{-1}], $I_2(\Theta)$ [s^{-2}] are the invariants of shear rate components Θ_{ij} [s^{-1}], n – dimensionless flow index depended on PL concentration in the biological fluid, $m=m$ (n,pH,T,We) – fluid consistency coefficient in Pas^n, e_{ijk} – tensor Levi-Civity, We-superficial layer wettability, pH – power hydrogen ion concentration. Geometrical non-linear relations between shear rate Θ_{ij} and biological fluid velocity components v_i [m/s] are as follows [29]:

$$\begin{aligned}\Theta_{ij}=\frac{1}{2}\left(v_{i|j}+v_{j|i}\right),\\ v_{i|j}\equiv\frac{1}{h_i}\left(\frac{\partial v_i}{\partial\alpha_j}-\frac{v_j}{h_i}\frac{\partial h_j}{\partial\alpha_i}+\delta_{ij}\sum_{k=1}^{3}\frac{v_k}{h_k}\frac{\partial h_j}{\partial\alpha_k}\right),\end{aligned} \tag{51}$$

where h_i – Lame coefficients.

References

[1] J. Cwanek, *The usability of the surface geometry parameters for the evaluation of the artificial hip joint wear*, Rzeszów University Press, Rzeszów, 2009.

[2] VC. Mow, A. Ratcliffe, and S. Woo, *Biomechanics of Diarthrodial Joints*, Springer Verlag, Berlin-Heidelberg-New York, 1990.

[3] K. Wierzcholski, "Time depended human hip joint lubrication for periodic motion with stochastic asymmetric density function", *Acta Bioeng. Biomech.* 16 (1), 83–97 (2014).

[4] O.S. Andersen and E. Roger, "Bilayer thickness and Membrane Protein Function: An Energetic Perspective", *Annu. Rev. Biophys. Biomolec. Struct.* 36 (1), 107–130 (2014).

[5] B. Bhushan, *Handbook of Micro/Nano Tribology*, second ed. CRC Press, Boca Raton, London, New York, Washington D.C., 1999.

[6] B. Bhushan, "Nanotribology and nanomechanics of MEMS/NEMS and BioMEMS/BioNEMS materials and devices", *Microelectron. Eng.* 84, 387–412 (2007).

[7] G. Chagnon, M. Rebouah, and D. Favier, "Hyperelastic Energy Densities for Soft Biological Tissues: A Review", *J. Elast.* 120 (2), 129–160 (2015).

[8] A. Gadomski, P. Bełdowski, J. Miguel Rubi, W. Urbaniak, K. Wayne, W.K. Auge, I.S. Holek, and Z. Pawlak, "Some conceptual thoughts toward nano-scale oriented friction in a model of articular cartilage", *Math. Biosci.* 244, 188–200 (2013).

[9] B.A. Hills, "Oligolamellar lubrication of joint by surface active phospholipid", *J. Reumatol.* 16, 82–91 (1989).

[10] B.A. Hills, "Boundary lubrication in vivo", *Proc. Inst. Mech. Eng. Part H-J. Eng. Med.* 214, 83–87 (2000).

[11] J. Marra and J.N. Israelachvili, "Direct measurements of forces between phosphatidylcholine and phosphatidylethanolamine bilayers in aqueous electrolyte solutions", *Biochemistry* 24, 4608–4618 (1985).

[12] Z. Pawlak, A. Gadomski, M. Sojka, W. Urbaniak, and P. Bełdowski, "The amphoteric effect on friction between the bovine cartilage/cartilage surfaces under slightly sheared hydration lubrication mode", *Colloids and Surfaces B: Biointerfaces* 1, 146, 452–458 (2016).

[13] Z. Pawlak, W. Urbaniak, and M.W. Hagner–Derengowska, "The Probable Explanation for the Low Friction of Natural Joints", *Cell Biochem. Biophys.* 71 (3), 1615–1621 (2015).

[14] Z. Pawlak, Z.A. Figaszewski, A. Gadomski, W. Urbaniak, and A. Oloyede, "The ultra–low friction of the articular surface is pH-dependent and is built on a hydrophobic underlay including a hypothesis on joint lubrication mechanism", *Tribol. Int.* 43, 1719–1725 (2010).

[15] Z. Pawlak, W. Urbaniak, A. Gadomski, Q. Kehinde, K.Q. Fusuf, I.O. Afara, and A. Oloyede, "The role of lamellate phospholipid bilayers in lubrication of joints", *Acta Bioeng. Biomech.* 14 (4), 101–106 (2012).

[16] Z. Pawlak, W. Urbaniak, and A. Oloyede, "The relationship between friction and wettability in aqueous environment of natural joints", *Wear* 271, 1745–1749 (2011).

[17] Z. Pawlak, A.D. Petelska, W. Urbaniak, K.Q. Fusuf, and A. Oloyede, "Relationship Between Wettability and Lubrication Characteristics of the Surfaces of Contacting Phospholipids-Based Membranes", *Cell Biochem. Biophys.* 65 (3), 335–345 (2012).

[18] A.D. Petelska and Z.A. Figaszewski, "Effect of pH on interfacial tension of bilayer lipid membrane", *Biophys. J.* 78, 812–817 (2000).

[19] I.M. Schwarz and B.A. Hills, "Synovial surfactant: Lamellar bodies in type B synoviocytes and proteolipid in synovial fluid and the articular lining", *Br. J. Rheumatol.* 35 (9), 821–827 (1966).

[20] A. Kucaba-Piętal, "Squeeze flow modelling with the use of micropolar fluid theory", *Bull. Pol. Ac.: Tech.* 65 (6), 927–933, (2017).

[21] K. Murawski and D. Lee, "Numerical methods of solving equations of hydrodynamics from perspectives of the code FLASH", *Bull. Pol. Ac.: Tech.* 59 (1), 927–933, (2011).

[22] K. Wierzcholski and A. Miszczak, "Mathematical principles and methods of biological surface lubrication with phospholipids bilayers", *Biosystems* 178, 32–40 (2019).

[23] K. Wierzcholski and A. Miszczak, "Electro-Magneto-Hydrodynamic Lubrication", *Open Phys.* 16 (1), 285–291 (2018).

[24] K. Wierzcholski, "Topology of calculating pressure and friction coefficients for time-dependent human hip joint lubrication", *Acta Bioeng. Biomech.* 13 (1), 41–56 (2011).

[25] M. Fisz, *Probability calculation and mathematical statistics*, PWN, Warszawa, 1967, [in Polish].

[26] Z. Helwig, *Elements of probability calculations and mathematical statistics*, PWN, Warszawa, 1977, [in Polish].

[27] C.Q. Yuan, Z. Peng, X.P. Yan, and X.C. Zhou, "Surface roughness evaluation in sliding wear process", *Wear* 265, 341–348 (2008).

[28] K. Wierzcholski, "Joint cartilage lubrication with phospholipids bilayer", *Tribologia* 2 (265), 145–157 (2016).

[29] P. Syrek, *Analiza parametrów przestrzennych aplikatorów małogabarytowych, wykorzystywanych w magnetoterapii*, Ph.D. thesis, AGH University of Sciences and Technology, Kraków 2011.